Materials and Design 77 (2015) 132–141

Contents lists available at ScienceDirect

Materials and Design

journal homepage: www.elsevier.com/locate/matdes

Foam filling radically enhances transverse shear response of corrugated sandwich plates

Bin Han [a,b], Bo Yu [a,b], Yu Xu [a,b], Chang-Qing Chen [c], Qian-Cheng Zhang [a,b,*], Tian Jian Lu [a,b,*]

[a] MOE Key Laboratory for Multifunctional Materials and Structures, Xi'an Jiaotong University, Xi'an 710049, PR China
[b] State Key Laboratory for Strength and Vibration of Mechanical Structures, Xi'an Jiaotong University, Xi'an 710049, PR China
[c] Department of Engineering Mechanics, CNMM & AML, Tsinghua University, Beijing 100084, PR China

ARTICLE INFO

Article history:
Received 6 January 2015
Revised 16 March 2015
Accepted 25 March 2015
Available online 25 March 2015

Keywords:
Corrugated sandwich core
Foam filling
Transverse shear
Collapse mode
Optimization

ABSTRACT

To improve the poor transverse shear resistance of corrugated sandwich cores, the present study uses a combined analytical and numerical approach to exploit the idea of filling core interstices with polymer foam. For foam-filled corrugated cores under transverse shear, four collapse modes are considered: elastic buckling, plastic buckling or yielding/fracture of corrugated strut, interfacial debonding/sealing off between corrugation platform and face sheets, and foam shear failure. Analytical models are constructed to determine the transverse shear stiffness and strength. To estimate the elastic/plastic buckling strength of a corrugated strut, the foam insertions are treated as a superposition of Winkler type elastic foundations to support the strut against buckling. Finite element simulations are carried out to validate the model predictions, with good agreement achieved. The sensitivity of transverse shear strength and failure mode to corrugation angle, strut slenderness and strain hardening of strut parent material is systematically studied; collapse mechanism map is constructed, and minimum weight design is carried out. Whether the sandwich is made of metal or fiber-reinforced composite, it is demonstrated that the foam-filled corrugated core exhibits radically enhanced transverse shear response, outperforming competing core topologies such as hollow pyramidal lattices and square honeycombs on the basis of equal mass.

1. Introduction

Lightweight sandwich constructions have gained structural preponderance over monolithic materials due to superior specific stiffness/strength and potential for multifunctional applications. The face sheets of a sandwich structure are typically made of metal or laminate composite, while the core is consisted of stochastic foam or periodic lattice structure such as truss and honeycomb. In recent years, there is also a growing interest in exploiting the stochastic foam as a filling material to enhance, simultaneously, the load-bearing and energy absorption capabilities of traditional lightweight structures, such as hollow tubes and sandwich constructions having flow-through, periodic lattice cores [1–6]. At present, existing studies on these foam-filled sandwiches have focused mainly on out-of-plane compression and three-point bending responses, both quasi-static and dynamic, which is important for understanding their blast resistance and indentation performance. However, shear response is of equal significance, as bending of the sandwich gives rise to transverse shear loading and to the possibility of collapse of the core in shear. Usually, core collapse in shear dominates the failure of sandwich beams and plates with thick cores and relatively thin face sheets.

Existing literature on the shear responses of various periodic lattice structures [7–12] demonstrated that while hollow/solid pyramidal lattices and honeycombs outperform corrugation lattices in transverse shear (loading direction aligned perpendicular to the prismatic direction), corrugations in longitudinal shear (loading direction aligned with the prismatic direction) may be comparable with pyramidal lattices and honeycombs. However, although corrugations may not be the best lattice topology in terms of mechanical stiffness/strength [10], corrugate-cored sandwich constructions have enjoyed widespread applications in areas of packaging, building and transportation industry (e.g., skin frame of high-speed trains and rocket engine shells), which is attributed mainly to their relatively low manufacturing costs. Under longitudinal shear, a corrugated sandwich core usually collapse with plastic shear wrinkling in cell walls [10], analogous to shear of honeycombs [11]; in comparison, under transverse shear, the

* Corresponding authors at: State Key Laboratory for Strength and Vibration of Mechanical Structures, Xi'an Jiaotong University, Xi'an 710049, PR China.
E-mail addresses: zqc111999@mail.xjtu.edu.cn (Z. Qian-Cheng), tjlu@mail.xjtu.edu.cn (L. Tian Jian).

http://dx.doi.org/10.1016/j.matdes.2015.03.050
0261-3069/

strength of the corrugated core is governed by Euler elastic/plastic buckling of the compressed constituent struts, similar in magnitude to that found under out-of-plane compression. Hence, the shear response of a corrugated core exhibits great anisotropy, poor in transverse shear and excellent in longitudinal shear.

As a kind of hybrid cellular structure, metallic corrugation filled with closed-cell metal foam has been investigated, both experimentally and numerically [6,13,14]. It is demonstrated that, when used as sandwich core, it exhibits superiority in both strength and energy absorption under quasi-static out-of-plane compression and transverse three-point bending over the traditional empty corrugated core. In addition, using finite element (FE) simulations, Vaziri et al. [1] assessed the effect of polymer foam filling on the mechanical properties of corrugated metallic sandwich plates. Foam-filled corrugated cores in longitudinal shear were found to have greater shear strength than equivalent unfilled ones, as foam filling effectively stabilized the corrugated struts against buckling. Nevertheless, thus far, no study focuses specifically on the transverse shear behavior of foam-filled corrugated cores. This deficiency will be addressed in the present study. We expect that inserting foams into the interstices of a corrugation may significantly enhance its transverse shear properties on the basis of equal mass.

This study is mainly focused upon how to accurately predict the equivalent transverse shear modulus and strength of polymer foam-filled corrugated sandwich cores in terms of corrugation topology and properties of constituent materials. In Section 2, upon specifying the problem, analytical models are developed for equivalent transverse shear modulus and strength that are dominated by four failure modes: *elastic buckling*, *plastic buckling* or *yielding/fracture* of corrugated struts, *interfacial debonding/sealing off* between corrugation platform and face sheets, and *foam shear failure*. To validate the prediction accuracy of the developed analytical models, FE models for foam-filled corrugated cores are constructed in Section 3. In Section 4, the influence of key geometrical parameters and strain hardening of strut parent material upon the transverse shear strength is discussed, and a collapse mechanism map is constructed. Consequently, minimum weight designs of the foam-filled corrugated core under transverse shear are given. Finally, the influence of strut parent material on minimum weight design is investigated, and the transverse shear strength of the foam-filled corrugated core is compared with competing topologies.

2. Analytical models

Fig. 1(a) and (b) presents schematically a foam-filled corrugated sandwich plate and the corresponding unit cell (foam insertion excluded for clarity), respectively. The sandwich structure is characterized by inclination angle θ, core web thickness t, length l, platform width f, core height $H = l\sin\theta + t$, and foam density ρ_f. Let the relative density $\bar{\rho}$ be defined as the ratio of the average density ρ_c of foam-filled corrugated core to the density ρ_s of corrugation material, as:

$$\bar{\rho} \equiv \rho_c/\rho_s = \lambda + (1-\lambda)\rho_f/\rho_s \tag{1}$$

where λ denotes the volume fraction of corrugation occupied by folded plates, given by [15]:

$$\lambda = \frac{(l+f)t}{(f+l\cos\theta)(t+l\sin\theta)} \tag{2}$$

Eq. (1) ignores the addition to mass by welding flux or adhesive glue, which is considered small relative to the mass of corrugation. Upon introducing two dimensionless parameters: $\alpha \equiv f/l$ and $\beta \equiv t/l$, λ can be rewritten as:

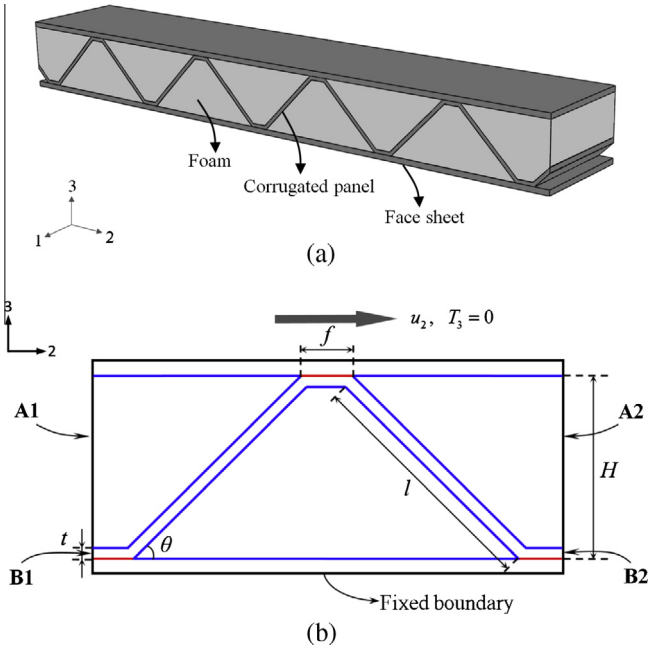

Fig. 1. Schematic of (a) foam-filled corrugated sandwich plate and (b) unit cell with additional details for finite element simulation: loading method, periodic boundary conditions, and interface condition. Red lines denote penalty contact and finite tangential sliding with the shear stress limit for failure prescribed as τ_b. Blue lines denote perfect bonding. (For interpretation of the references to color in this figure legend, the reader is referred to the web version of this article.)

$$\lambda = \frac{(1+\alpha)\beta}{(\alpha+\cos\theta)(\beta+\sin\theta)} \tag{3}$$

which, in the limit of vanishing platform volume, reduces to that obtained by Côté et al. [10]:

$$\lambda = \frac{2\beta}{\sin 2\theta} \tag{4}$$

The transverse shear response of an empty or foam-filled corrugated sandwich core may be simplified as a planar deformation problem. Thus, a corrugated panel with small t/l is taken as an inclined strut fully bonded to the face sheets which, under pure shear loading, may be treated as a rigid body, with no rotation at both ends. Hence, its ends may be treated as clamped, as confirmed by FE simulations (see later). It is further assumed that the foam and the corrugated panel are perfectly bonded at the interfaces, so that close contact with each other is maintained during deformation and there is no slipping at the interface.

To facilitate theoretical modeling, an idealized unit cell model is considered, as shown in Fig. 1(b). With planar deformation assumed, plane strain deformation prevails so that the corrugated panel has effective Young's modulus $\bar{E}_s = E_s/(1-\nu^2)$ and yield stress $\bar{\sigma}_Y = 2\sigma_Y/\sqrt{3}$. Similarly, the foam insertion has effective Young's modulus $\bar{E}_f = E_f/(1-\nu_f^2)$. Here, E_s, ν and σ_Y denote the Young's modulus, Poisson ratio and yielding stress of the core web material, while E_f, ν_f and τ_{fc} denote the Young's modulus, Poisson ratio and shear strength of the foam material, respectively.

2.1. Equivalent shear modulus

With reference to Fig. 1, the equivalent transverse shear modulus G_{23} of the foam-filled corrugated core may be obtained by superposition of the contributions from corrugation and foam [1], as:

$$G_{23} = \frac{\overline{E}_s \beta \sin(2\theta)(1+\beta/\sin\theta)}{2(1+\alpha/\cos\theta)} + (1-\lambda)G_f = \widetilde{G}_s + \widetilde{G}_f \tag{5}$$

where G_f is the shear modulus of the foam material and $\widetilde{G}_f$ represents the contribution of foam alone. The equivalent transverse shear modulus of the empty corrugated core, $\widetilde{G}_s$, is derived from the principle of force balance that considers only the stretching deformation of the core web.

Alternatively, the equivalent elastic constants of a foam-filled corrugated core can be obtained by applying the homogenization method based upon the principle of energy equivalence [16]. Thus, as an alternative to Eq. (5) derived by superposition, the equivalent transverse shear modulus is expressed as:

$$\begin{aligned} G_{23} &= \left(\frac{1}{2}\overline{E}_s \beta \sin(2\theta) + \frac{1}{2}\overline{E}_s \beta^3 \frac{\cos^2(2\theta)}{\sin(2\theta)} + 2\nu\beta G_f \sin(2\theta)\right)\frac{(1+\beta/\sin\theta)}{(1+\alpha/\cos\theta)} \\ &\quad + (1-\lambda)G_f \\ &= \left(\widetilde{G}_s + \widetilde{G}_b + \widetilde{G}_c\right) + \widetilde{G}_f \end{aligned} \tag{6}$$

where $\widetilde{G}_b$ is the contribution by core web bending and $\widetilde{G}_c$ is attributed to the coupling effect between foam insertion and core web. The difference between Eqs. (5) and (6) is the additional consideration of core web bending as well as coupling contribution induced by the lateral stress that develops by foam matrix in shear stressing as a result of core web deformation due to the Poisson ratio effect.

To evaluate the influence of foam insertion (both individual contribution and coupling effect) and core web bending, Fig. 2 plots the equivalent transverse shear modulus of a foam-filled corrugated core as a function of corrugation angle. For comparison, results for an empty corrugated core having identical geometric configuration are included. Two typical foam materials, a polymer foam (Rohacell WF51) and a close-celled aluminum foam with porosity 76%, are considered, representing separately soft and rigid foams. It is seen from Fig. 2 that foam contribution is obvious only when G_f/E_s is sufficiently large (e.g., aluminum foam filling), and that the contribution of core web bending only arises at large t/l and $\theta < 10^\circ$ (or $\theta > 80^\circ$). Further, contribution by the coupling effect is so faint that it may be ignored even if a rigid foam such as aluminum foam is inserted. Consequently, with contributions from both core web bending and coupling effect neglected, the simple formula (5) is sufficiently accurate for the prediction of equivalent transverse shear modulus.

The results of Fig. 2 suggest that filling a metallic corrugated core with foam could not effectively increase its transverse shear modulus. Further, Fig. 2 implies that the optimal corrugation angle maximizing the transverse shear modulus of a foam-filled corrugated core is about 45°, almost the same as that of an empty corrugated core.

Given the transverse shear modulus results shown in Fig. 2, the scope of subsequent analysis on the transverse shear strength of a foam-filled corrugated core is restricted to geometric configurations satisfying $0.0001 \leqslant t/l \leqslant 0.2$ and $10^\circ \leqslant \theta \leqslant 80^\circ$. For such configurations, the bending deformation of core webs as well as the coupling effect between core web and foam insertion can be safely ignored. Hence, only the stretching deformation of core webs needs to be taken into account in the strength analysis.

2.2. Transverse shear strength

Du et al. [17,18] investigated experimentally the shear and bending properties of *X–Z*-pin reinforced polymethacrylimide (PMI) foam-cored sandwich constructions, and found that pin reinforcement enhanced effectively the shear stiffness and strength of the sandwich. However, under shear loading, it was observed that the failure of a *Z*-pin foam-cored sandwich corresponded to the shear failure of foam, with crack initiation and propagation at small strain levels. Thus, for the present foam-filled corrugated cores, it is expected that foam shear failure is also likely to occur. On the other hand, debonding at the interface of the core and face sheets is prone to occur for a sandwich plate under shear loading. For a foam-filled corrugated sandwich or a foam-cored sandwich (without corrugations), high strength epoxy adhesive is commonly chosen to bond the foam to the core webs and face sheets, both having much larger shear strength than the foam. Therefore, debonding at the interface between the foam and core web or face sheets is usually posterior to foam shear failure, and hence may be ignored.

For the present corrugate-cored sandwich construction, corrugated panels are typically manufactured first using the folding process for metal panels or the molding prepreg technology for composite laminates [19], which are then connected to the face sheets by braze welding or adhesive bonding. Consequently, debonding or sealing off at the interface between the platform of corrugation and the face sheets is likely to occur due to limited bonding or welding area. This scenario is taken into account in the strength analysis.

In consequence, different from the relatively simple strength analysis of Vaziri et al. [1] for foam-filled corrugated sandwich plates under transverse shear, the present study considers four types of failure mode: (a) elastic buckling of corrugated struts; (b) plastic buckling, yielding or fracture of corrugated struts; (c) debonding of interface between corrugation platform and face sheets; and (d) foam shear failure. The following assumptions are made:

1. The face sheets are rigid in comparison with the relatively compliant foam-filled core. The influence of shear deformation of the face sheets on shear stiffness and strength of the sandwich is neglected.
2. Strain in the foam insertion is pure shear, and equal during deformation before failure occurs. For simplicity, the foam experiencing pure shear straining fails with elastic–brittle fracture: when the maximum shear stress in the foam reaches its strength τ_{fc}, the foam fails and the integrity of the foam-filled corrugated core is lost [20].
3. Shear stress at the interface between the platform of corrugation and the face sheets is uniformly distributed.
4. The strength analysis of a foam-filled corrugated sandwich plates subjected to transverse shear is based upon small deformation. Within a unit cell, the axial stresses and strains of two adjacent corrugated struts are equal in magnitude but opposite in sign, namely, one in compression and the other in tension.

If the disturbance in strain due to the presence of struts is ignored for the foam insertions, the transverse shear strength of a foam-filled core may be expressed as:

$$\tau^p = \sigma_{cr}\frac{\beta\cos\theta}{(\alpha+\cos\theta)} + (1-\lambda)\tau_f \tag{7}$$

where τ_f is the average shear stress in the foam insertions, and σ_{cr} is the axial compressive stress of the corrugated struts corresponding to (any type of) failure once it occurs.

2.2.1. Buckling or yielding/fracture of corrugated struts

Under axial compressive loading, buckling is prone to occur for corrugated struts, especially for slender struts. Foam insertions added to the interstices of a corrugated core can greatly enhance the buckling resistance of the struts. To determine the critical buckling stress of a corrugated strut surrounded by the filling

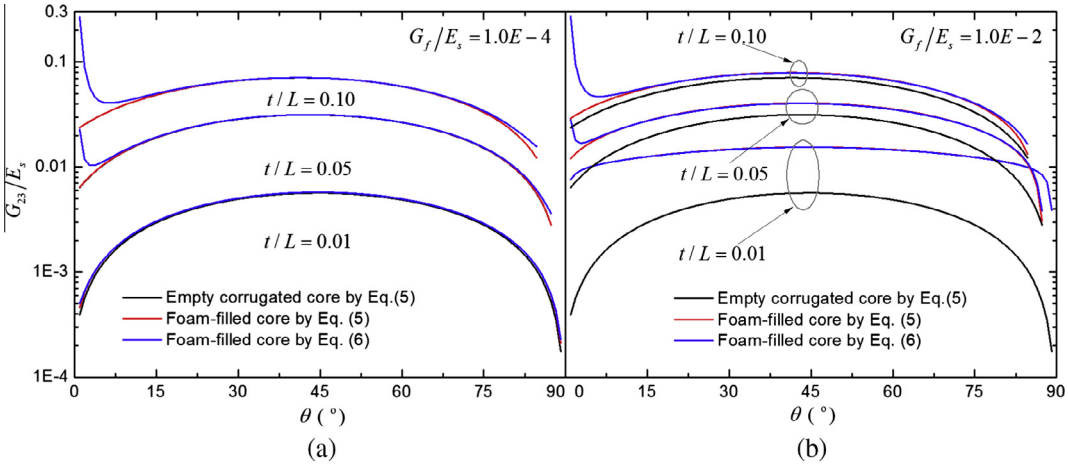

Fig. 2. Transverse shear modulus of foam-filled corrugated sandwich core plotted as a function of corrugation angle ($\alpha = 0.1$): (a) filled with soft foam (e.g., Rohacell WF51); (b) filled with rigid foam (e.g. close-celled aluminum foam with porosity 76% [14]).

foam, it is modeled as a column resting on an equivalent Winkler elastic foundation (see Appendix B). As shown in Appendix A, the elastic buckling stress of a straight inclined bar resting on Winkler elastic foundation with simply supported or clamped end-constraints is given as:

$$\sigma_{cr} = \begin{cases} \sqrt{\frac{\bar{E}_f \bar{E}_s \beta}{3}\left(\frac{\cos\theta}{\sin\theta+\beta} + \frac{\sin\theta}{\cos\theta+\alpha}\right)}, & \text{simply supported ends} \\ \frac{\pi^2 \bar{E}_s \beta^2}{3} + \sqrt{\frac{\bar{E}_f \bar{E}_s \beta}{3}\left(\frac{\cos\theta}{\sin\theta+\beta} + \frac{\sin\theta}{\cos\theta+\alpha}\right)}, & \text{clamped ends} \end{cases} \tag{8}$$

For a corrugated sandwich core as shown in Fig. 1(b), it is reasonable to assume the struts are clamped, which is validated by FE calculations in Section 3. Thus, if the parent material of the corrugated struts exhibits elastic ideally plastic or elastic–brittle fracture response, the critical compressive stress of the strut is given by:

$$\sigma_{cr} = \begin{cases} \frac{\pi^2 \bar{E}_s \beta^2}{3} + \sqrt{\frac{\bar{E}_f \bar{E}_s \beta}{3}\left(\frac{\cos\theta}{\sin\theta+\beta} + \frac{\sin\theta}{\cos\theta+\alpha}\right)}, & \text{if } \sigma_{cr} < \bar{\sigma}_Y \\ \bar{\sigma}_Y, & \text{otherwise} \end{cases} \tag{9}$$

However, in case of an elastic plastic hardening parent material, the critical compressive stress for elastic or plastic buckling of the strut is given by the elastic buckling and Shanley plastic bifurcation stresses [21], as:

$$\sigma_{cr} = \begin{cases} \frac{\pi^2 \bar{E}_s \beta^2}{3} + \sqrt{\frac{\bar{E}_f \bar{E}_s \beta}{3}\left(\frac{\cos\theta}{\sin\theta+\beta} + \frac{\sin\theta}{\cos\theta+\alpha}\right)}, & \text{if } \sigma_{cr} < \bar{\sigma}_Y \\ \frac{\pi^2 E_t \beta^2}{3} + \sqrt{\frac{\bar{E}_f E_t \beta}{3}\left(\frac{\cos\theta}{\sin\theta+\beta} + \frac{\sin\theta}{\cos\theta+\alpha}\right)}, & \text{otherwise} \end{cases} \tag{10}$$

where $E_t \equiv d\sigma/d\varepsilon$ is the tangent modulus of the plane strain true stress versus true strain curve of the material evaluated at σ_{cr}. To obtain the plastic buckling stress with Eq. (10) evaluated at various points along the material data curve until the buckling stress equals the material stress σ_{cr}, an iterative process is necessary.

With small deformation assumption, the macroscopic shear strain may be expressed using the axial stretching strain $\varepsilon_{\text{axial}}$ of the corrugated struts, as:

$$\gamma = \frac{\varepsilon_{\text{axial}}}{\cos\theta(\sin\theta+\beta)} \tag{11}$$

where

$$\varepsilon_{\text{axial}} = \begin{cases} \sigma_{cr}/\bar{E}_s, & \text{when } \sigma_{cr} \leqslant \bar{\sigma}_Y \\ \varepsilon(\sigma_{cr}), & \text{otherwise} \end{cases} \tag{12}$$

Assuming equal strain in the foam-filled core, one has $\gamma = \gamma_f$, where γ_f is shear strain in the foam. Shear stress in the foam can thence be calculated as:

$$\tau_f = G_f \gamma \tag{13}$$

Finally, the transverse shear strength of the foam-filled corrugated core corresponding to the failure mode of strut buckling or yielding/fracture may be obtained by inserting Eqs. (9) or (10), together with Eqs. (11)–(13), into Eq. (7).

2.2.2. Shear failure of foam

When shear failure of foam occurs prior to other failure modes, one has $\tau_f = \tau_{fc}$. If the corrugated struts are in elastic state, the shear strength may be obtained using Eq. (5) as:

$$\tau^p = G_{23}\frac{\tau_{fc}}{G_f} \tag{14}$$

However, when the strut parent material is elastic plastic hardening, the above formula cannot be used if the stress in the strut exceeds the elastic limit of the material when the foam fails. Rather, from Eqs. (11) and (13), one obtains:

$$\varepsilon_{\text{axial}} = \cos\theta(\sin\theta+\beta)\tau_{fc}/G_f \tag{15}$$

Correspondingly, the plastic axial compressive stress of the corrugated struts may be obtained from the material data curve $\sigma_{cr} = \sigma_{cr}(\varepsilon_{\text{axial}})$. Eventually, the transverse shear strength of the foam-filled core is calculated using Eq. (7).

2.2.3. Debonding/sealing off of interface between corrugation platform and face sheets

Interfacial debonding/sealing off is a common failure mode for sandwich plates under shear. This failure mode is expected when the interfacial shearing stress in the bonding or welding region exceeds the bond adhesion or welding strength τ_b. It is assumed that the interfacial shearing stress is induced only by stretching/compression of the inclined struts, rather than shearing of the filling foam.

The interfacial shear stress is assumed to be constant along the length of the corrugation platform, satisfying:

$$\tau_b f = 2\sigma_{cr} t \cos\theta \tag{16}$$

Eq. (16) may not be very realistic as many simplifications are involved, but is still the basis for evaluating adhesive shear strength in many test standards such as ASTM and ISO [22]. The axial stress of the corrugated struts follows from (16) as:

$$\sigma_{cr} = \frac{\tau_b \alpha}{2\beta \cos\theta} \tag{17}$$

The transverse shear strength of the foam-filled core corresponding to debonding/sealing off is obtained by inserting Eqs. (11)–(13) and (17) into (7).

3. Finite element simulations

3.1. Finite element model

To verify the accuracy/rationality of the analytical predictions detailed in the previous section, two-dimensional (2D) FE simulations are carried out using the implicit solver of commercial FE code ABAQUS (version 6.10). The foam-filled corrugated core (including the corrugated struts) is modeled using four-noded plane strain quadrilateral elements with reduced integration (CPE4R). Both the top and bottom face-sheets are taken as rigid, as no deformation of the face-sheets is assumed.

A mesh consisting of approximately square elements with size $l/50$ is employed to model the filling foam. For the corrugated struts (including the platform), a mesh of rectangular elements with size $t/6$ across the thickness and size $H/50$ along the axial direction is employed. Numerical experimentation confirms that such mesh choices lead to a response almost independent of mesh size.

As shown in Fig. 1(b), perfect bonding at either the foam/face-sheet or foam/strut interface is assumed. To simulate the possible collapse mode of *sealing off* or *debonding* at the interface between corrugation platform and top/bottom face-sheet, the interface is modeled using surface-to-surface contacts under the penalty contact method and finite tangential sliding, with the stress limit for shear failure prescribed as τ_b.

A single unit of the foam-filled corrugated core is employed as the representative volume element (RVE), with periodic boundary conditions applied on its vertical edges (A_1, A_2) and (B_1, B_2) as shown in Fig. 1(b). Let (u_{i1}, u_{i2}) denote the displacements of points (nodes) on edges (A_1, A_2) and (B_1, B_2), where $i = 1, 2$. The following relationships are prescribed for each pair of nodes on edges (A_1, A_2) and (B_1, B_2):

$$u_{i1} - u_{i2} = 0, \quad i = 1, 2 \tag{18}$$

except for the 4 corner nodes that are also contained in the top and bottom face-sheets, which are required to satisfy the prescribed boundary conditions.

The bottom face-sheet is fixed. While the rotation of the top face-sheet is constrained, it can translate in direction 3, implying that the normal traction $T_3 = 0$; see Fig. 1(b). To model pure transverse shear loading, a translation displacement u_2 along direction 2 is prescribed on the top face-sheet.

It should be pointed out that no geometric imperfections are introduced into the present 2D FE model, since the lack of symmetry about the centroid of either the empty or foam-filled corrugated core is sufficient to induce a preferential buckling direction of the sandwich structure.

Table 1
Mechanical properties of (a) polymer foam and (b) base material of corrugated strut.

Material (a) Foam	Density ρ_f (g/cm^3)	Young's modulus E_f(MPa)	Poisson ratio v_f	Shear strength τ_{fc} (MPa)
Rohacell 31 (R31)	0.031	36	0.2	0.3
Rohacell 51 (R51)	0.051	70	0.3	0.8
H100	0.1	120	0.32	1.6
H200	0.2	280	0.32	3.3
(b) Base material	ρ_s(g/cm^3)	E_s (GPa)	v	Compressive strength[a] σ_Y (MPa)
304 stainless steel	7.90	210	0.3	210
Ti–6Al–4V	4.43	114	0.33	1070
GFRP	1.77	30	0.18	350
CFRP	1.55	110	0.32	870

[a] Mechanical properties of 304 stainless steel, Ti–6Al–4V and GFRP are taken from Liu et al. [23], while those of CFRP from Li et al. [24]. CFRP refers to unidirectional carbon fiber reinforced composite materials (T700/3234). Compression strength σ_Y of 304 stainless steel refers to its yielding strength (plastic hardening should be consider when the stress exceeds σ_Y). For Ti–6Al–4V, GFRP and CFRP, σ_Y denotes the compression crushing strength.

3.2. Comparison between numerical and analytical predictions

FE calculations are performed for a sandwich plate having a 304 stainless steel corrugated core filled with PMI foam (Rohacell 51, see Table 1). The ratio of corrugation platform length to strut length is fixed at $\alpha = 0.1$, and the inclination of corrugation fixed at $\theta = 45^\circ$ which is typically chosen in previous research [11,24,25]. The 304 stainless steel is taken as an elastic plastic hardening material with Young's modulus $E_s = 210$ GPa, linear hardening tangent modulus $E_t = 2$ GPa, Poisson ratio $v = 0.3$ and initial yield strength $\sigma_Y = 210$ MPa. To study the effect of plastic hardening, the case of 304 stainless steel without plastic hardening ($E_t = 0$) is also considered. It is assumed that the corrugation platform and the face sheets are connected through brazing with a shear strength $\tau_b = 120$ MPa [25]. For simplicity, Rohacell 51 is taken as a linear elastic material. The distribution of shear stress in the foam is extracted from the FE model, and the load at which the maximum shear stress first exceeds the foam shear strength τ_{fc} is taken as the load of foam shear failure.

The numerically calculated normalized transverse shear strength (namely, specific shear strength) $\tau^p/\bar{\rho}\sigma_Y$ is plotted in Fig. 4 as a function of strut slenderness ratio β and compared with that analytically predicted. Good agreement is achieved, either the 304 stainless steel exhibits strain hardening or not, confirming the accuracy of the present analytical models. The various collapse modes of the foam-filled corrugated core appearing in Fig. 4 will be discussed in the next section.

4. Results and discussions

This section presents firstly systematic results concerning the influence of geometric parameters (i.e., corrugation angle θ and slenderness ratio β) as well as strain hardening of the strut parent material upon the transverse shear strength of a 304 stainless steel corrugated core filled with Rohacell 51 foam. Collapse mechanism maps are subsequently constructed and minimum weight designs given. Finally, the transverse shear strength of the foam-filled corrugated core is compared with competing topologies on the basis of equal mass.

4.1. Influence of geometric parameters

Consider first the effect of corrugation angle. Fig. 3 plots the specific shear strength as a function of corrugation angle for $\alpha = 0.1$ and a range of relative densities. Results obtained with strain hardening ($E_t = 2$ GPa) for 304 stainless steel are compared with those without strain hardening ($E_t = 0$). Generally, the foam-filled core with corrugation angle $\theta = 45^\circ$ has the maximum specific shear strength. The maximum specific shear strength increases with increasing relative density when $\bar{\rho} \leqslant 0.10$, for which the collapse of the core is dominated by elastic or plastic buckling of the corrugated struts. More specifically, foam-filled cores with $\bar{\rho} < 0.015$ collapse by *elastic buckling*, and the degree of strain hardening has no effect on the shear strength. For foam-filled cores satisfying $0.015 \leqslant \bar{\rho} \leqslant 0.10$, *plastic buckling* of corrugated struts occurs. However, when the foam relative density is increased further (i.e., $\bar{\rho} > 0.10$), the collapse mode of the core is transformed into *foam shear failure* or *interfacial sealing off* between corrugation platform and face sheets. In addition, the critical angle corresponding to the maximum specific shear strength is shifted towards 90°, and the maximum specific shear strength decreases with increasing $\bar{\rho}$. It is worth noting that, with $\bar{\rho} \geqslant 0.15$, *foam shear failure* occurs for relatively small corrugation angles (struts in elastic state) and relatively high corrugation angles (struts in plastic hardening state), while *interfacial sealing off* happens for intermediate corrugation angles satisfying $15^\circ < \theta < 55^\circ$. Here, the maximum specific shear strength usually occurs at the corrugation angle separating the collapse modes of *interfacial sealing off* and *foam shear failure*.

The effect of strut slenderness ratio β on specific shear strength is considered next for a foam-filled core of $\alpha = 0.1$ and $\theta = 45^\circ$. The results presented in Fig. 4 suggest that, as β is increased from 0.001 to 0.1, the collapse mode of the core is determined successively by *elastic buckling*, *plastic buckling of struts*, *foam shear failure* and *sealing off*. Compared with the case with no strain hardening ($E_t = 0$), strain hardening of 304 stainless steel affects the collapse modes of *plastic buckling*, *foam shear failure* and part of *sealing off*: when these collapse modes occur, the corrugated struts are all in plastic hardening state. Overall, the normalized shear strength increases with β, until $\beta \approx 0.06$ which corresponds to the transition of collapse mode from *foam shear failure* to *sealing off*. At this stage, as the ratio of corrugation platform length to strut length is fixed at 0.1, which limits the force resisting interfacial sealing off/debonding, the specific shear strength starts to decrease; see Fig. 4.

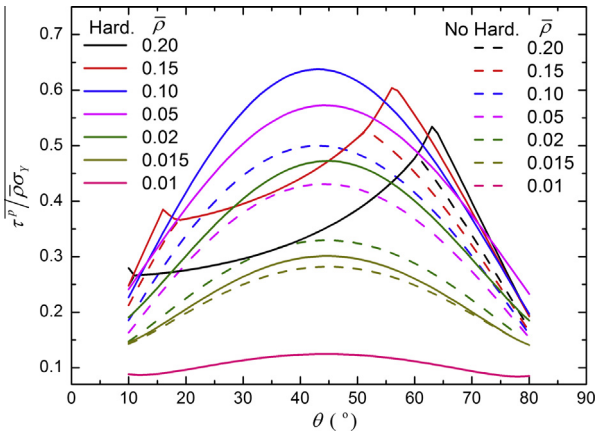

Fig. 3. Influence of corrugation angle upon normalized transverse shear strength of R51 foam-filled corrugated core ($\alpha = 0.1$), with each line representing a given relative density. Solid lines denote cases with strain hardening of 304 stainless steel considered (abbreviated as Hard.), while dash lines denote those without considering strain hardening (abbreviated as No Hard.).

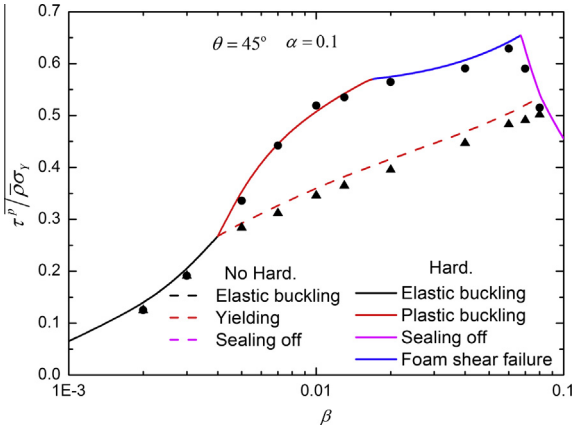

Fig. 4. Effect of strut slenderness ratio β on normalized transverse shear strength of R51 foam-filled corrugated core ($\theta = 45^\circ$ and $\alpha = 0.1$). Both strain hardening and no hardening of 304 stainless steel are considered. Solid lines denote cases with strain hardening of 304 stainless steel considered (abbreviated as Hard.), while dash dot lines denote those without considering strain hardening (abbreviated as No Hard.). Solid circles denote numerical results with strain hardening of 304 stainless steel considered, while solid triangles denote numerical results without considering strain hardening.

4.2. Collapse mechanism map

Using the analytical expressions of Section 2.2, we construct failure mechanism maps in terms of nondimensional geometric parameters, $\alpha = f/l$ and $\beta = t/l$, for sandwich cores composed of strain hardening 304 stainless steel and Rohacell 51 foam filler under transverse shear. A typical failure mechanism map for the case of $\theta = 45^\circ$ is presented in Fig. 5, which not only gives a visual representation of failure but also makes it easier to identify the operative collapse mode for a given core geometry. For the purpose of selecting minimum weight geometries for a given load index τ^p, contours of relative density $\bar{\rho}$ and shear strength τ^p are superimposed onto the collapse map. As shown in Fig. 5, the path of minimum weight designs moves along the boundary between *sealing off* and its adjacent failure modes.

4.3. Minimum weight design

In this section, under a given critical transverse shear load index τ^p, minimum weight design is carried out for foam-filled corrugated sandwich cores using the present analytical predictions.

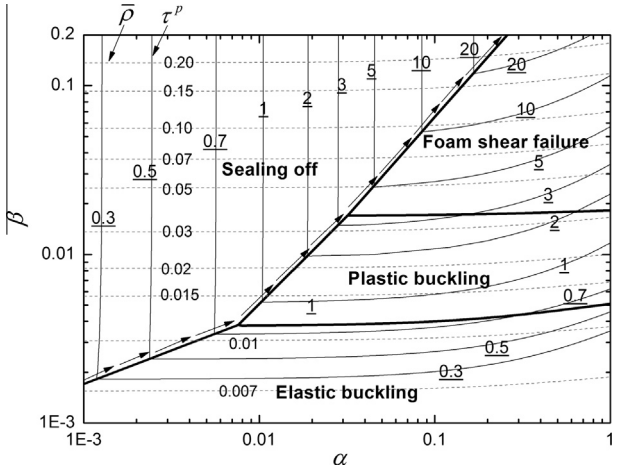

Fig. 5. Collapse mechanism map for 304 stainless steel corrugated core ($\theta = 45^\circ$) filled with Rohacell 51 foam under transverse shear, with contours of relative density $\bar{\rho}$ and shear strength τ^p added. The arrows trace the path of minimum weight designs with increasing τ^p.

Specifically, geometric parameters α, β and θ are chosen as the design variables, which are varied over the design space to obtain a minimum weight solution at each loading index. For a sandwich core having specified constituent materials, its relative density $\bar{\rho}$ (as the mass index) is minimized for a given τ^p subjected to the constraints that none of the failure modes detailed in Section 2.2 occurs. The optimization problem is solved using the sequential quadratic programming (SQP) algorithm coded in MATLAB.

For foam-filled corrugated cores composed of strain hardening 304 stainless steel and polymer foam (with its density varying as R31, R51, H100 and H200; see Table 1), Figs. 6(a–d) present separately the optimized loading paths of minimum weight and the corresponding geometric parameters. The optimization is performed by imposing limits on the thickness of corrugated struts, namely, $0.001 \leqslant \beta \leqslant 0.2$, which are chosen for ease of fabrication.

It is seen from Fig. 6(a) that corrugated cores filled with R31 and R51 foams are structurally more efficient than empty corrugated cores. In sharp contrast, the structural efficiency of corrugated cores filled with H100 and H200 foams is inferior to the corresponding empty cores. In other words, under transverse shear, it is beneficial to fill the interstices of a strain hardening 304 stainless steel corrugated core with a relatively weak (low density) polymer foam. Additionally, the superiority of R31/R51-filled corrugated cores over the empty ones is especially obvious at low load levels ($\tau^p < 3$ MPa), where the optimal path is governed by simultaneous *elastic buckling* and *sealing off*. As the load index is increased, the advantage of foam filling gradually diminishes, accompanied by collapse mode transition from *elastic buckling* to *plastic buckling* or *foam shear failure*, similar to the out-of-plane compressive behavior of foam-filled corrugated cores [14].

The values of α, β and θ corresponding to the minimum weight design of Fig. 6(a) are presented in Fig. 6(b–d). While the non-dimensional platform length α varies nearly linear with the load index for relatively weak foams (R31, R51 and H100) or empty corrugation, the difference in non-dimensional strut thickness β (as well as α) for different foam-filled sandwich cores including empty ones decreases as the load index is increased. The corrugation angle θ varies within a small range between 41.7° and 45°, and the optimal corrugation angle for an empty core is smaller than that of a foam-filled core. Generally, the optimal core topology is governed by simultaneous *elastic buckling* and *sealing off* for lightly loaded sandwiches, by the confluence of *plastic buckling* and *sealing off* for moderately loaded sandwiches, and by the confluence of *foam shear failure* and *sealing off* for heavily loaded sandwiches.

4.4. Performance comparison

4.4.1. Comparison with competing topologies

The transverse shear strength of optimized R51 foam-filled corrugated cores is compared with other competing lattice structures as shown in Fig. 7 where, for consistence, all the lattice structures are made of strain hardening 304 stainless steel. The results of Fig. 7 clearly demonstrate that, on the basis of equal mass, foam-filled corrugated cores exhibit dramatically improved transverse shear response over empty corrugations and diamond lattices [10], X-type truss lattices [26], WBK truss lattices [27], and square honeycombs [11], and are even slightly superior over optimized hollow and solid pyramidal lattices [12]. This finding is significant as corrugate-cored sandwich structures are commonly found in a variety of engineering applications.

4.4.2. Material selection for corrugated struts

Except for 304 stainless steel, the design of a foam-filled corrugated sandwich core can be extended to a wide variety of materials for the corrugated struts. Fig. 8 plots the transverse shear strength of an optimized R51 foam-filled corrugated core as a function of core density for selected parent materials of corrugation, including Ti–6Al–4V, woven glass fiber reinforced plastic (GFRP), carbon

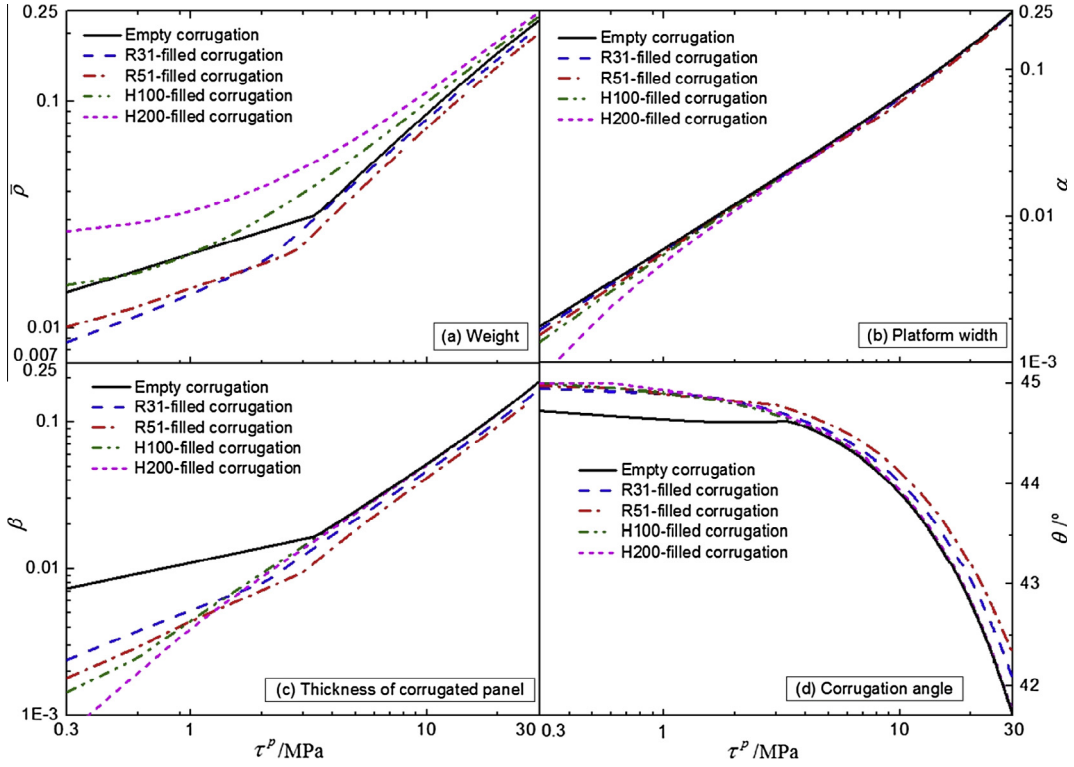

Fig. 6. Minimum weight design in transverse shear: (a) comparison between foam-filled corrugated cores and empty ones; (b) optimal corrugation platform width normalized by strut length; (c) optimal strut thickness normalized by strut length; and (d) optimal corrugation angle. Corrugated struts are made of 304 stainless steel with strain hardening ($E_t = 2.1$ GPa); polymer foam fillers have four densities (R31, R51, H100 and H200).

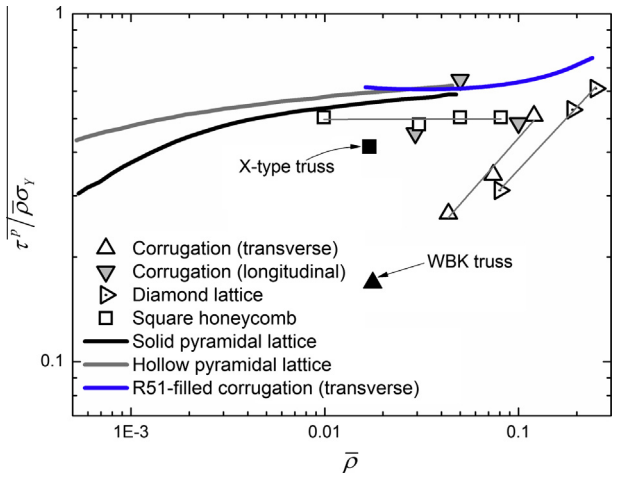

Fig. 7. Normalized shear strength of lattice structures (all made of strain hardening 304 stainless steel) plotted as a function of relative density $\bar{\rho}$ (core density normalized by density of 304 stainless steel). Solid and hollow pyramidal lattices refer to truss struts with solid or hollow circular section [12]. Data for empty corrugated cores in both longitudinal and transverse shear and diamond lattices in transverse shear are taken from Côté et al. [10]; those of square honeycombs from Côté et al. [11], X-type truss lattice from Zhang et al. [26], and WBK truss lattice from Lee et al. [27]. Results of Rohacell 51 (R51) foam-filled corrugations are obtained by the present study. Bold lines refer to finite element results. Discrete data points represent experimental results.

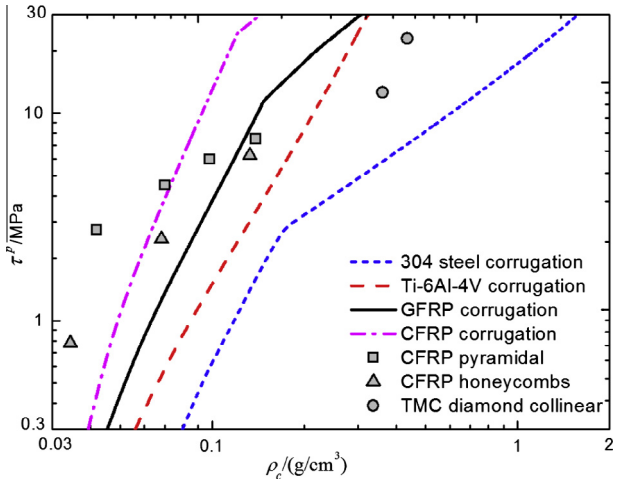

Fig. 8. Comparison of minimum weight designs of foam-filled corrugated sandwich cores made of different strut parent materials. 304 steel, Ti–6Al–4V, GFRP and CFRP corrugation denote separately Rohacell 51 (R51) foam-filled 304 stainless steel ($E_t = 2.1$ GPa), Ti–6Al–4V, glass fiber reinforced composite (GFRP), and carbon fiber reinforced composite (CFRP) corrugated cores. Data taken from [7] for CFRP pyramidal, honeycomb and TMC diamond collinear are included for further comparison.

fiber reinforced plastic (CFRP), and 304 stainless steel (as reference). Relevant properties of these materials are summarized in Table 1. In the case of Ti–6Al–4V, GFRP, or CFRP, it is assumed that the corrugation platform and the face sheets are connected using adhesive bonding, with a typical adhesive shear strength of $\tau_b = 35$ MPa. Simultaneously, existing data for sandwich plates having CFRP pyramidal, honeycomb, and TMC diamond collinear cores, which have thus far enjoyed nearly the best shear strength [7], are added to Fig. 8 for comparison.

The results of Fig. 8 demonstrate that, under transverse shear, foam-filled cores made of Ti–6Al–4V, GFRP, or CFRP corrugated struts perform considerably better than those made of 304

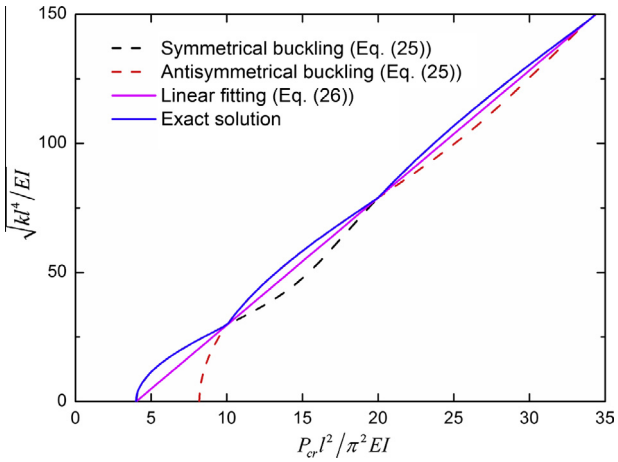

Fig. A1. A graph of $\sqrt{kl^4/EI}$ versus $P_{cr}l^2/(\pi^2 EI)$ relation for an initially straight bar with fixed ends.

stainless steel, as the parent strut material of the former has higher specific elastic modulus (E/ρ) and higher specific strength (σ_Y/ρ). In other words, in addition to foam filling, increasing the specific elastic modulus and specific strength (yielding or fracture) of the strut parent material leads to further enhanced shear performance. Moreover, when $\rho_c > 0.06$ g/cm^3, it is seen from Fig. 8 that R51 foam-filled CFRP corrugated cores even outperform CFRP pyramidal, honeycomb, and TMC diamond collinear cores.

5. Conclusions

The idea of using foaming filling to enhance the poor transverse shear performance of a corrugated sandwich core has been theoretically exploited. The main findings are summarized as follows:

(1) Filling a corrugated steel sandwich core with polymer foam leads to radically enhanced transverse shear strength that surpasses even the best known cellular sandwich cores (square honeycombs and hollow pyramidal lattices). On the basis of equal mass, the enhancement increases with decreasing foam relative density.
(2) The superiority of foam-filled corrugated cores over empty (unfilled) ones is more obvious at relatively low load levels where sandwich collapse is dominated by strut elastic buckling.
(3) For corrugated struts made of 304 stainless steel, the specific shear strength is sensitive to corrugation angle and strut slenderness ratio. Strain hardening of strut parent material only affects the shear strength in the case of moderate slenderness ratios where collapse is accompanied by strut yielding.
(4) Under transverse shear, sandwiches with polymer foam-filled CFRP corrugated cores are superior to those having CFRP pyramidal, CFRP honeycomb and TMC diamond collinear lattice cores on equal mass basis.

Acknowledgments

This work was supported by the National Basic Research Program of China (2011CB610305), the National Natural Science Foundation of China (11472209 and 11472208), the National 111 Project of China (B06024), and the Shaanxi Province 13115 Project.

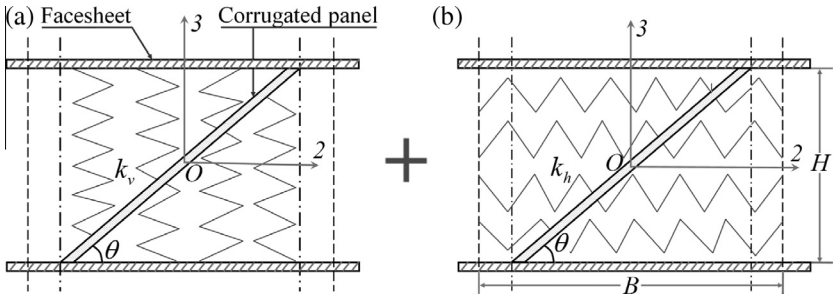

Fig. B1. Winkler type elastic foundation model for foam-filled corrugated core: (a) vertical springs with spring coefficient k_v; and (b) horizontal springs with spring coefficient k_h.

Appendix A. Stability of Initially Straight Beams Resting on Winkler Elastic Foundation

For an initially straight beam resting on a Winkler foundation, the differential governing equation may be written as [28]:

$$EI\frac{d^4w}{dx^4}+P\frac{d^2w}{dx^2}+kw=0 \tag{A1}$$

where w and EI are the lateral displacement and flexural rigidity of the beam, k is the equivalent spring coefficient of the Winkler foundation, and P is the axial end force. The corresponding general solution for a beam with length l is:

$$w=A\sin\frac{\phi_1 x}{l}+B\cos\frac{\phi_1 x}{l}+C\sin\frac{\phi_2 x}{l}+D\cos\frac{\phi_2 x}{l} \tag{A2}$$

where A, B, C and D are arbitrary constants, and $\left\{\begin{matrix}\phi_1\\ \phi_2\end{matrix}\right\}=\sqrt{\frac{\gamma_1}{2}\pm\sqrt{\left(\frac{\gamma_1}{2}\right)^2-\gamma_2}}$, $\gamma_1=Pl^2/EI$ and $\gamma_2=kl^4/EI$ being dimensionless parameters.

For a beam with torsional spring restraints at the two ends, the boundary conditions may be written as:

$$\begin{aligned} &x=0,\ w=0,\ w'=-M_1/\alpha_1\\ &x=l,\ w=0,\ w'=M_2/\alpha_2 \end{aligned} \tag{A3}$$

where α_1 and α_2 are the stiffness of the torsional springs at the two ends of the beam; M_1 and M_2 are the corresponding bending moments at the ends.

Inserting Eq. (A2) into Eq. (A3) leads to a quaternary system of homogeneous linear equations, as:

$$\begin{bmatrix} 0 & 1 & 0 & 1\\ \phi_1 & \lambda_1\phi_1^2 & \phi_2 & \lambda_1\phi_2^2\\ \sin\phi_1 & \cos\phi_1 & \sin\phi_2 & \cos\phi_2\\ \phi_1\cos\phi_1-\lambda_2\phi_1^2\sin\phi_1 & -\phi_1\sin\phi_1-\lambda_2\phi_1^2\cos\phi_1 & \phi_2\cos\phi_2-\lambda_2\phi_2^2\sin\phi_2 & -\phi_2\sin\phi_2-\lambda_2\phi_2^2\cos\phi_2 \end{bmatrix}\begin{Bmatrix} A\\ B\\ C\\ D\end{Bmatrix}=0 \tag{A4}$$

where $\lambda_1=EI/\alpha_1 l$ and $\lambda_2=EI/\alpha_2 l$. By setting the determinant of coefficient matrix of Eq. (A4) to zero, the nondimensional load parameter γ_1 and the critical load P_{cr} are obtained.

For a beam simply supported at the two ends ($M_1=M_2=0$), its elastic buckling load is [29]:

$$P_{cr}=n^2\frac{\pi^2 EI}{l^2}+\frac{1}{n^2}\frac{kl^2}{\pi^2} \tag{A5}$$

The critical load corresponding to the smallest P_{cr} can be written as:

$$P_{cr_{\min}}=2\sqrt{kEI} \tag{A6}$$

For a beam clamped at both ends ($\alpha_1\to\infty$ and $\alpha_2\to\infty$), the characteristic equation is given by [28]:

$$\begin{aligned} &\phi_1\tan\phi_1=\phi_2\tan\phi_2, && \text{for symmetric buckling}\\ &\phi_1\cot\phi_1=\phi_2\cot\phi_2, && \text{for anti-symmetric buckling} \end{aligned} \tag{A7}$$

The numerical solution of Eq. (A7) can be found with great accuracy by Newton iteration. Alternatively, the buckling load for any fixed-end beam with finite length may be expressed with good approximation as:

$$P_{cr_{\min}}=4\frac{\pi^2 EI}{l^2}+2\sqrt{kEI} \tag{A8}$$

As shown in Fig. A1, the discrepancy between (A7) and (A8) is small, especially for large $\sqrt{kl^4/EI}$. Consequently, in the present study, Eq. (A8) is employed for analytical modeling.

Appendix B. Equivalent Winkler Model for Foam-filled Corrugated Sandwich Cores

To determine the buckling stress of a corrugated (inclined) strut, following Liu et al. [23], the foam insertions are treated as a superposition of two Winkler type elastic foundations to support the strut, assuming the constraints from the foam is uniformly distributed. As shown in Fig. B1(a), in the first foundation model, a strut of width W and thickness t is supported by vertical springs with spring coefficient k_v. To a good approximation, this coefficient may be written as:

$$k_v=\frac{\overline{E}_f W}{H}=\frac{\overline{E}_f W}{l\sin\theta+t} \tag{B1}$$

In the second foundation model as shown in Fig. B1(b), the strut is placed on horizontal springs with spring coefficient k_h. By invoking the periodic boundary conditions, k_h may be calculated as:

$$k_h = \frac{\overline{E}_f W}{B} = \frac{\overline{E}_f W}{l\cos\theta + f} \tag{B2}$$

where B refers to the width of half unit cell. The total foundation modulus is therefore given by:

$$k = k_v \cos\theta + k_h \sin\theta = \overline{E}_f \frac{W}{l}\left(\frac{\cos\theta}{\sin\theta+\beta} + \frac{\sin\theta}{\cos\theta+\alpha}\right) \tag{B3}$$

Finally, upon inserting Eq. (B3) into Eqs. (A6) or (A8), the buckling stress for a compressed corrugated strut supported by foam filling may be obtained with $\sigma_{cr} = P_{cr_{\min}}/tW$.

References

[1] A. Vaziri, Z. Xue, J.W. Hutchinson, Metal sandwich plates with polymer foam-filled cores, J. Mech. Mater. Struct. 1 (2006) 95–125.
[2] A.G. Mamalis, D.E. Manolakos, M.B. Ioannidis, K.N. Spentzas, S. Koutroubakis, Static axial collapse of foam-filled steel thin-walled rectangular tubes: experimental and numerical simulation, Int. J. Crashworthines 13 (2008) 117–126.
[3] A.A. Nia, M.Z. Sadeghi, The effects of foam filling on compressive response of hexagonal cell aluminum honeycombs under axial loading-experimental study, Mater. Des. 31 (2010) 1216–1230.
[4] J.B. Ostos, R.G. Rinaldi, C.M. Hammetter, G.D. Stucky, F.W. Zok, A.J. Jacobsen, Deformation stabilization of lattice structures via foam addition, Acta Mater. 60 (2012) 6476–6485.
[5] J. Zhang, P. Supernak, S. Mueller-Alander, C.H. Wang, Improving the bending strength and energy absorption of corrugated sandwich composite structure, Mater. Des. 52 (2013) 767–773.
[6] L.L. Yan, B. Yu, B. Han, C.Q. Chen, Q.C. Zhang, T.J. Lu, Compressive strength and energy absorption of sandwich panels with aluminum foam-filled corrugated cores, Compos. Sci. Technol. 86 (2013) 142–148.
[7] P. Moongkhamklang, V.S. Deshpande, H.N.G. Wadley, The compressive and shear response of titanium matrix composite lattice structures, Acta Mater. 58 (2010) 2822–2835.
[8] T. George, V.S. Deshpande, H.N.G. Wadley, Mechanical response of carbon fiber composite sandwich panels with pyramidal truss cores, Compos. Part A-Appl. Sci. 47 (2013) 31–40.
[9] B.P. Russell, V.S. Deshpande, H.N.G. Wadley, Quasistatic deformation and failure modes of composite square honeycombs, J. Mech. Mater. Struct. 3 (2008) 1315–1340.
[10] F. Côté, V.S. Deshpande, N.A. Fleck, A.G. Evans, The compressive and shear responses of corrugated and diamond lattice materials, Int. J. Solids Struct. 43 (2006) 6220–6242.
[11] F. Côté, V.S. Deshpande, N.A. Fleck, The shear response of metallic square honeycombs, J. Mech. Mater. Struct. 1 (2006) 1281–1299.
[12] S.M. Pingle, N.A. Fleck, V.S. Deshpande, H.N.G. Wadley, Collapse mechanism maps for the hollow pyramidal core of a sandwich panel under transverse shear, Int. J. Solids Struct. 48 (2011) 3417–3430.
[13] L.L. Yan, B. Han, B. Yu, C.Q. Chen, Q.C. Zhang, T.J. Lu, Three-point bending of sandwich beams with aluminum foam-filled corrugated cores, Mater. Des. 60 (2014) 510–519.
[14] B. Han, L.L. Yan, B. Yu, Q.C. Zhang, C.Q. Chen, T.J. Lu, Collapse mechanisms of metallic sandwich structures with aluminum foam-filled corrugated cores, J. Mech. Mater. Struct. 9 (2014) 397–425.
[15] H.N.G. Wadley, Multifunctional periodic cellular metals, Philos. Trans. R. Soc. A 364 (2006) 31–68.
[16] B. Han, K.K. Qin, B. Yu, Q.C. Zhang, C.Q. Chen, T.J. Lu, Design optimization of foam-reinforced corrugated sandwich beams. Compos. Struct. (2015), submitted for publication.
[17] L. Du, G. Jiao, T. Huang, L. Zhao, F. Huang, Shear properties of X-Z-pin reinforced foam core sandwich, Acta Mater. Compos. Sin. 24 (2007) 140–146.
[18] L. Du, G. Jiao, T. Huang, Investigation of the effect of Z-pin reinforcement on the collapse of foam-cored sandwich panels, J. Reinf. Plast. Compos. 27 (2008) 1211–1224.
[19] S. Kazemahvazi, D. Tanner, D. Zenkert, Corrugated all-composite sandwich structures-Part 2: failure mechanisms and experimental programme, Compos. Sci. Technol. 69 (2009) 920–925.
[20] A. Mostafa, K. Shankar, E.V. Morozov, Insight into the shear behavior of composite sandwich panels with foam core, Mater. Des. 50 (2013) 92–101.
[21] F.R. Shanley, Inelastic column theory, J. Aeronaut. Sci. 14 (1947) 261–268.
[22] L.F.M. da Silva, P.J.C. das Neves, R.D. Adams, J.K. Spelt, Analytical models of adhesively bonded joints-Part I: Literature survey, Int. J. Adhes. Adhes. 29 (2009) 319–330.
[23] T. Liu, Z.C. Deng, T.J. Lu, Analytical modeling and finite element simulation of the plastic collapse of sandwich beams with pin-reinforced foam cores, Int. J. Solids Struct. 45 (2008) 5127–5151.
[24] M. Li, L.Z. Wu, L. Ma, B. Wang, Z.X. Guan, Structural response of all-composite pyramidal truss core sandwich columns in end compression, Compos. Struct. 93 (2011) 1964–1972.
[25] S.T. Liu, K.Z. Yang, Effect of holding time and brazing temperature on microstructure and mechanical properties of 304 stainless steel brazed joints, Hot Working Technol. 40 (2011) 172–174.
[26] Q.C. Zhang, Y.J. Han, C.Q. Chen, T.J. Lu, Ultralight X-type lattice sandwich structure (I): concept, fabrication and experimental characterization, Sci. China Ser. E 52 (8) (2009) 2147–2154.
[27] Y.H. Lee, J.E. Choi, K.J. Kang, A wire-woven cellular metal: Part-II, evaluation by experiments and numerical simulations, Mater. Des. 30 (2009) 4459–4468.
[28] Z.P. Bazant, L. Cedolin, Stability of Structures: Elastic, Inelastic, Fracture and Damage Theories, Oxford University Press, New York, 1991.
[29] S.P. Timoshenko, J.M. Gere, Theory of Elastic Stability, McGraw-Hill, New York, 1961.